DRAFT VERSION FEBRUARY 5, 2008
Preprint typeset using LaTeX style emulateapj v. 04/03/99

GRAVITATIONAL BENDING OF LIGHT NEAR COMPACT OBJECTS

ANDREI M. BELOBORODOV[1]
Canadian Institute for Theoretical Astrophysics, University of Toronto, 60 St. George Street, Toronto, ON M5S 3H8, Canada

Draft version February 5, 2008

ABSTRACT

A photon emitted near a compact object at an angle α with respect to the radial direction escapes to infinity at a different angle $\psi > \alpha$. This bending of light is caused by a strong gravitational field. We show that, in a Schwarzschild metric, the effect is described by $1-\cos\alpha = (1-\cos\psi)(1-r_g/R)$ where R/r_g is the emission radius in Schwarzschild units. The formula is approximate and it applies at $R \geq 2r_g$ only, however at these radii it has amazing accuracy, fully sufficient in many applications. As one application we develop a new formulation for the light bending effects in pulsars. It reveals the simple character of these effects and gives their quantitative description with practically no losses of accuracy (for the typical radius of a neutron star $R = 3r_g$ the error is 1%). The visible fraction of a star surface is shown to be $S_v/4\pi R^2 = [2(1-r_g/R)]^{-1}$ which is $3/4$ for $R = 3r_g$. The instantaneous flux of a pulsar comes from one or two antipodal polar caps that rotate in the visible zone. The pulse produced by one blackbody cap is found to be sinusoidal (light bending impacts the pulse amplitude but not its shape). When both caps are visible, the pulse shows a plateau: the variable parts of the antipodal emissions precisely cancel each other. The pulsed fraction of blackbody emission with antipodal symmetry has an upper limit $A_{\max} = (R-2r_g)/(R+2r_g)$. Pulsars with $A > A_{\max}$ must be asymmetric.

Subject headings: gravitation — radiation mechanisms: general — relativity — stars: neutron — (stars:) pulsars: general — X-rays: binaries

1. INTRODUCTION

Light bending by gravity is a classical effect of general relativity (e.g. Misner, Thorne, & Wheeler 1973). In a spherically symmetric gravitational field, the exact bending angle is given by an elliptic integral (see Appendix). The effect plays important role in astrophysics; e.g. weak bending gives rise to the gravitational lensing phenomenon. Strong bending occurs near compact objects (black holes and neutron stars) and crucially affects their emission.

In this Letter we give a simple formula for the bending angle that replaces the elliptic integral with high accuracy at radii $R \geq 2r_g$. Here $r_g = 2GM/c^2$ is the Schwarzschild radius of the gravitating spherical object of mass M. We apply this formula to neutron stars and develop a new simple formalism for the light bending effects in pulsars. We illustrate with pulsars that have two point-like antipodal spots emitting thermal radiation, and compare the results with the exact theory (Pechenick, Ftaclas, & Cohen 1983). The advantage of our formalism is that it gives a clear understanding of the bending effects and describes them analytically with almost no losses of accuracy as long as stars with $R > 2r_g$ are considered. The exact theory well describes stars with any R, including $R < 2r_g$ where the bending angle β can exceed 90°, however it requires a complicated numerical treatment. Standard models of neutron stars predict $R > 2r_g$ with a typical $R \approx 3r_g$ (e.g. Shapiro & Teukolsky 1983). Our formalism then works with $\sim 1\%$ accuracy and should be sufficient in many practical problems. It should also be good for accretion disks around Schwarzschild black holes: the disk inner edge is at $3r_g$ and the bulk of emitted radiation does not enter the region $R < 2r_g$.

[1]Also at Stockholm Observatory, SE-106 91 Stockholm, Sweden and Astro-Space Center of LPI, Profsojuznaja 84/32, Moscow 117810, Russia

2. THE COSINE RELATION

Let an emitter be located at point E at a radius R (Fig. 1). A photon emitted along the radial direction escapes radially. A photon emitted at some angle α with respect to radius (α is measured by the local observer at E) escapes along a bent trajectory. We will describe the trajectory in polar coordinates (r,ψ) where $\psi = 0$ for the escape direction. The standard way of computing $\alpha(\psi)$ is given in Appendix. Instead one can use the approximate relation

$$1-\cos\alpha = (1-\cos\psi)\left(1-\frac{r_g}{R}\right). \qquad (1)$$

The accuracy of relation (1) is remarkably high. It gives the bending angle $\beta = \psi - \alpha$ with a small fractional error $e = \delta\beta/\beta$ shown in Figure 2. For example for $R = 3r_g$ the maximum error is $e_{\max} = 3\%$ (at $\alpha = 90^\circ$) and $e < 1\%$ for $\alpha < 75^\circ$. High accuracy is maintained for $R > 2r_g$. For $R < 2r_g$ the approximation is not applicable: then $\cos\alpha = 0$ would correspond to $\cos\psi < -1$. We therefore limit our consideration to radiation escaping from $R > 2r_g$ where $\beta < 90^\circ$.

The high accuracy of equation (1) is a striking property of the Schwarzschild spacetime. This functional shape cannot be understood as a linear expansion in r_g/R (that expansion is given in Appendix and its accuracy is much worse). Equation (1) can be understood as follows. Let us consider $x = 1-\cos\alpha$ as a small parameter and expand $y = 1-\cos\psi$ in terms of x^k. After some algebra we find

$$y = \frac{x}{1-u} - u^2\left[\frac{1}{112}\left(\frac{x}{1-u}\right)^3 + \frac{1}{224}\left(\frac{5}{3}-u\right)\left(\frac{x}{1-u}\right)^4 + O(x^5)\right], \quad (2)$$

where $u = r_g/R$. The linear term is just equation (1); it describes the standard solid angle transformation $d\Omega_0 = 2\pi dx \to d\Omega = 2\pi dy$ along the radial ray. The interesting property of equation (2) is that the x^2-term vanishes and the higher order terms have small coefficients. It explains the extremely high accuracy of equation (1) at small u and/or x (Fig. 1). Only when both $x \to 1$ and $u \to 0.5$ there is a sizable correction to the linear term and here e peaks sharply. The linear expansion in u (also derived in Appendix) reads $y = x(1+u) + O(u^2)$.

Though the cosine relation (1) is sufficient for our subsequent discussion, note that it also gives a simple description for the shape of a photon trajectory with a given impact parameter b (Fig. 1). Equation (1) can be written at any point (r, ψ) along the trajectory if α measures the angle between the photon velocity and the local radial direction. Combining (1) with (10) we find $r^2 = b^2[\sin^2\psi + (1-\cos\psi)^2 r_g/r]^{-1}$ and

$$r(\psi) = \left[\frac{r_g^2(1-\cos\psi)^2}{4(1+\cos\psi)^2} + \frac{b^2}{\sin^2\psi}\right]^{1/2} - \frac{r_g(1-\cos\psi)}{2(1+\cos\psi)}. \quad (3)$$

Trajectories (3) are very close to the exact ones. The fractional error of r at a given ψ is $\delta r/r < 4\times 10^{-3}$ as long as $r > 2r_g$.

3. THE VISIBLE SURFACE OF A STAR AND THE OBSERVED FLUX

Consider a spherical compact star viewed by an observer at distance $D \gg R$. Choose spherical coordinates (R, ψ, ϕ) with the polar axis $\psi = 0$ directed toward the observer. What is the observed flux dF from a surface element dS of the star? First of all one should decide whether dS is visible. In a flat spacetime the visibility condition would be simply $\mu = \cos\psi > 0$ where ψ is the polar angle of dS. The star gravity creates curvature that allows the observer to see regions with negative μ down to a critical μ_v that defines the dark side of the star. The observed light from the circle $\mu = \mu_v$ is emitted tangentially to the star ($\alpha = 90^o$). Exact calculations of $\alpha(\psi)$ via the elliptic integral yield tabulated μ_v, e.g. $\mu_v = -0.886, -0.633, -0.484$ for $R/r_g = 2, 2.5, 3$. From equation (1) we find immediately the approximate $\mu_v = -r_g/(R-r_g)$. The visible fraction of the surface is $S_v/4\pi R^2 = (1-\mu_v)/2 = [2(1-r_g/R)]^{-1}$, e.g. we get 0.75 for $R = 3r_g$ while the exact value is 0.742.

Appendix gives the standard formula for the observed flux from a visible dS (eq. 11). It requires the knowledge of $\alpha(\psi)$ and the exact theory leads to a complicated numerical treatment of the problem (Pechenick et al. 1983). Instead we use the approximate equation (1); then equation (11) reads

$$dF = \left(1 - \frac{r_g}{R}\right)^2 I_0(\alpha)\cos\alpha\frac{dS}{D^2}, \quad (4)$$

where $\cos\alpha = \mu(1-r_g/R) + r_g/R$. Equation (4) is surprisingly simple. Apart from the redshift factor $(1-r_g/R)^2$ the element dS emits as if the problem were Newtonian with ψ replaced by α.

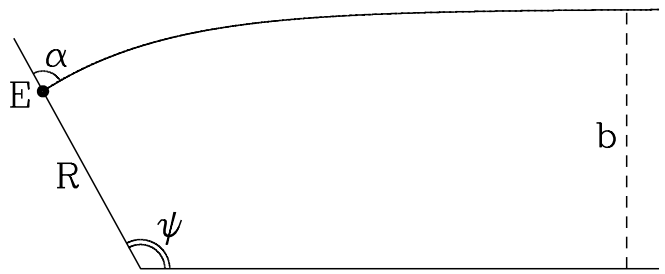

FIG. 1.— Example photon trajectory. The emission point E is at $R = 2.5r_g$ and the emission angle is $\cos\alpha = 0.1$; the corresponding impact parameter $b = 3.21r_g$. In this case $\cos\psi = -0.482$ and the bending angle $\beta = \psi - \alpha \approx 35^o$. The approximate trajectory (eq. 3) is also plotted here and it is not distinguishable from the exact trajectory.

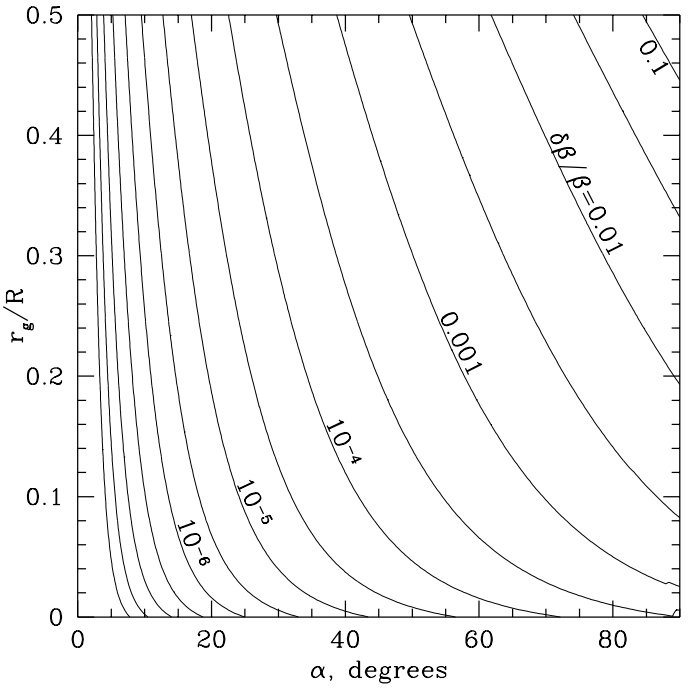

FIG. 2.— Accuracy of the cosine relation (1). This relation gives the bendig angle $\beta = \psi - \alpha$ with an error $e = \delta\beta/\beta$ which depends on the emission radius R/r_g and the emission angle α. Here the contours of $e = const$ (with logarithmic step 0.5) are plotted on the $r_g/R - \alpha$ plane.

When the local intensity of radiation $I_0(\alpha)$ is known for all dS, equation (4) can be integrated over the visible surface $\mu > \mu_v$ to get the total observed flux. For example, suppose a star has a homogeneous hot spot of arbitrary size and shape that emits thermal radiation [$I_0(\alpha) = const$]. Denote the spot area by $s = \int dS$ and the corresponding projected area by $s_\perp = \int \mu dS$ (if only a part of the spot is in the visible zone $\mu > \mu_v$ the integrals are taken over this part). Then the observed flux is $F = (I_0/D^2)(1-r_g/R)^2[s_\perp(1-r_g/R) + sr_g/R]$. Note that $s_\perp < 0$ when the spot is in the region $\mu_v < \mu < 0$.

4. PULSARS

Consider a neutron star with two antipodal hot spots associated with polar caps of the star magnetic field. Assume here that the spot size is small compared to the star radius R. The star is spinning and its magnetic axis is inclined to the spin axis by an angle $\theta \leq 90^{\rm o}$. Therefore the spots periodically change their position and inclination with respect to a distant observer and the observed radiation pulsates.

The spot whose circle of rotation is closer to the observer will be called "primary" and the other symmetric spot "antipodal". Denote the unit vector pointing toward the observer by $\mathbf{d}$ and the angle between $\mathbf{d}$ and the spin axis by i. To compute the radiation fluxes from the primary and antipodal spots one needs to know their inclinations: $\mu = \mathbf{n}\cdot\mathbf{d}$ and $\bar{\mu} = \bar{\mathbf{n}}\cdot\mathbf{d}$, where $\mathbf{n}$ and $\bar{\mathbf{n}} = -\mathbf{n}$ are the spot normals. When the star executes its rotation, μ varies periodically between $\mu_{\rm min} = \cos(i+\theta)$ and $\mu_{\rm max} = \cos(i-\theta)$,

$$\mu(t) = \sin\theta\sin i\cos\Omega t + \cos\theta\cos i. \qquad (5)$$

Here Ω is the angular velocity of the pulsar; $t = 0$ is chosen when $\mu = \mu_{\rm max}$.

Consider the blackbody component of the pulsar emission; it has isotropic intensity $I_0(\alpha) = const$. Using (4) we find the observed fluxes F and $\bar{F}$ from the primary and antipodal spots (when they are visible)

$$\frac{F}{F_1} = \mu\left(1-\frac{r_g}{R}\right)+\frac{r_g}{R}, \quad \frac{\bar{F}}{F_1} = -\mu\left(1-\frac{r_g}{R}\right)+\frac{r_g}{R}. \qquad (6)$$

Here $F_1 = (1-r_g/R)^2 I_0 s/D^2$, s is the spot area, and point-like-spot approximation is adopted. For the antipodal spot we substituted $\bar{\mu} = -\mu$. The observer sees the primary spot when $\mu > \mu_v$ and the antipodal spot when $\bar{\mu} > \mu_v$ (§ 3). Denote $\kappa = r_g/(R-r_g) = |\mu_v|$. Both spots are seen when $-\kappa < \mu < \kappa$ and then the observed flux is

$$F_{\rm obs} = F + \bar{F} = 2\frac{r_g}{R}F_1 = const \ ! \qquad (7)$$

Hence the blackbody pulse must display a plateau whenever both spots are in the visible zone. We emphasize the high accuracy of equations (6) and (7), though the exact theory does not give the ideal plateau. The fractional error δ in $F_{\rm obs}$ is maximal when $\mu = \mu_v$, e.g. $\delta_{\rm max} \approx 1.3\%$ for $R = 3r_g$. For $R = 2r_g$ our formalism predicts that the whole surface is visible and $F_{\rm obs}$ is given by equation (7) at any θ, i, μ; then $\delta_{\rm max} \approx 6\%$.

At any time $F_{\rm obs}$ takes one of three values: F, $\bar{F}$, or $F+\bar{F}$. A pulsar shows the plateau (7) if $\cos(i+\theta) < \kappa$. A pulsar with arbitrary i and θ belongs to one of four classes described in Figures 3 and 4. It is easy to compute the pulsed fraction $A = (F_{\rm max}-F_{\rm min})/(F_{\rm max}+F_{\rm min})$ for each class,

$$A = \begin{cases} (\mu_{\rm max}-\mu_{\rm min})/(\mu_{\rm max}+\mu_{\rm min}+2\kappa) & \text{class I} \\ (\mu_{\rm max}-\kappa)/(\mu_{\rm max}+3\kappa) & \text{class II, III} \\ 0 & \text{class IV} \end{cases} \qquad (8)$$

A reaches its maximum $A_{\rm max}$ if the pulsar has $\mu_{\rm max} = 1$ and $\mu_{\rm min} < \kappa$. This maximum is $A_{\rm max} = (R-2r_g)/(R+2r_g)$.

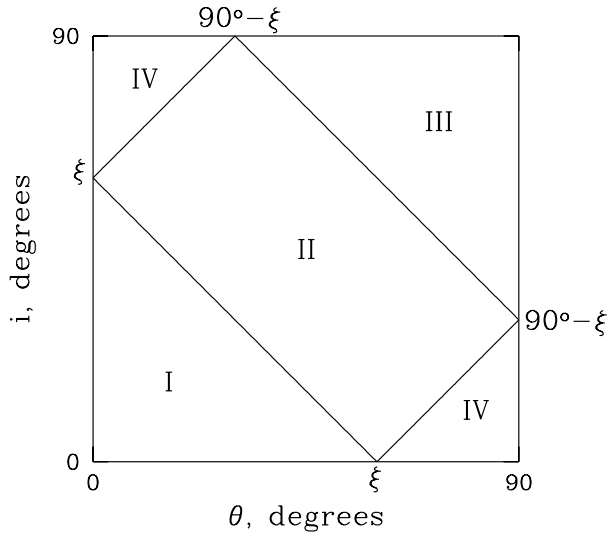

FIG. 3.— Location of classes I–IV on the $i-\theta$ plane. The angle ξ is defined so that $\cos\xi = r_g/(R-r_g)$, e.g. $\xi = 60^{\rm o}$ for $R = 3r_g$. The classes are determined by the relative positions of $\mu_{\rm min} = \cos(i+\theta)$, $\mu_{\rm max} = \cos(i-\theta)$, $\kappa \equiv r_g/(R-r_g)$, and $-\kappa$. **Class I**: $\mu_{\rm min} > \kappa$. The antipodal spot is never seen in such a pulsar (and the primary spot is visible all the time). The observed blackbody pulse has a perfect sinusoidal shape. **Class II**: $-\kappa < \mu_{\rm min} < \kappa < \mu_{\rm max}$. The primary spot is seen all the time and the antipodal spot also appears for some time. The pulse has a sinusoidal profile $F(t)$ interrupted by the plateau (7). **Class III**: $\mu_{\rm min} < -\kappa$. The primary spot is not visible for a fraction of period (and then only the antipodal spot is seen). Such a pulsar shows a primary sinusoidal profile $F(t)$ interrupted by the plateau (7) and the plateau is interrupted by a weaker sinusoidal sub-pulse $\bar{F}(t)$ from the antipodal spot. The sub-pulse occurs when only the antipodal spot is in the visible zone. **Class IV**: $-\kappa < \mu_{\rm min}, \mu_{\rm max} < \kappa$. Both spots are seen at any time. Then the observed blackbody flux is constant (eq. 7). Only anisotropic emission with $I_0(\alpha) \neq const$ can contribute to pulsations.

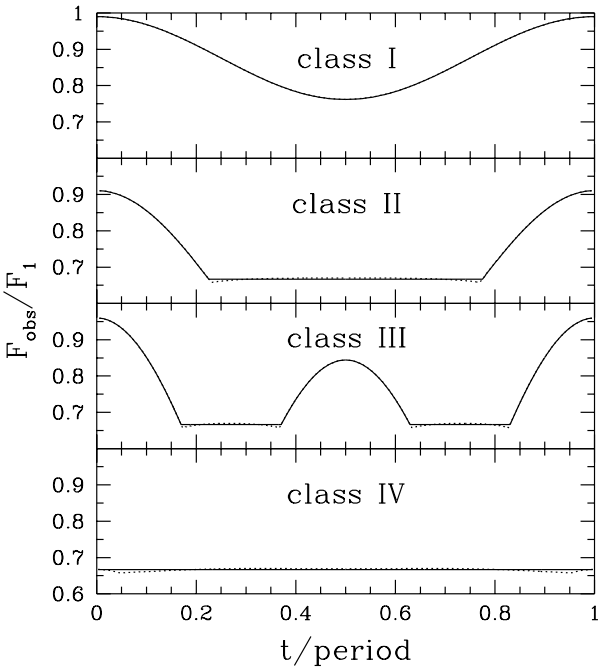

FIG. 4.— Blackbody pulse profiles for classes I–IV defined in Fig. 3. $R = 3r_g$ is chosen and the flux is normalized to F_1 (the maximum possible flux that is observed when the primary spot is viewed face on). Class I is exemplified with $\theta = 20^{\rm o}$ and $i = 30^{\rm o}$, class II with $\theta = 30^{\rm o}$ and $i = 60^{\rm o}$, class III with $\theta = 60^{\rm o}$ and $i = 80^{\rm o}$, and class IV with $\theta = 20^{\rm o}$ and $i = 80^{\rm o}$. The approximate model developed in this paper is shown by solid curves and the exact model is shown by dotted curves. The plateau has the same level in all cases: $F_p/F_1 = 2r_g/R = 2/3$.

5. CONCLUSIONS

A new formulation for the light bending effect is given in this Letter. It makes use of an approximate simple formula that describes photon trajectories with remarkable accuracy (eq. 1).

This formulation is applied to pulsars where light bending is known to be a crucial effect. The developed analytical theory replaces the previously used complicated numerical treatment with high accuracy, sufficient for practical purposes. For example, it immediately gives the observed pulse profile for a rotating neutron star with two antipodal hot spots (eqs. 6 and 7). These analytical expressions highlight the effects of light bending in pulsars: (i) If the antipodal spot is never seen, the blackbody pulse is perfectly sinusoidal. The bending affects the pulsed fraction A only (eq. 8). (ii) The visible surface of the star is significantly enhanced, $S_v/4\pi R^2 = [2(1-r_g/R)]^{-1}$, and both spots may be seen for a fraction of period or all the time. Then the blackbody pulse shows a plateau $F_{\rm obs} = F_p = (2r_g/R)F_1$ where F_1 is the flux from one spot viewed face on. (iii) The observed flux cannot exceed F_1 and it cannot be smaller than F_p. The latter is a purely relativistic effect: $F_p = 0$ in the Newtonian limit $r_g/R \to 0$. The maximum pulsed fraction of a pulsar with antipodal symmetry is $A_{\max} = (F_1 - F_p)/(F_1 + F_p) = (R - 2r_g)/(R + 2r_g)$. This is a severe constraint, e.g. $A_{\max} = 1/5$ for $R = 3r_g$ instead of Newtonian $A_{\max} = 1$.

Within a few percent the results agree with the previous numerical works. The new formalism, however, is much simpler in use. It gives a clear description of the pulse profiles for given i, θ, and R/r_g and makes it easier to compare the theory with observations and constrain pulsar parameters. We focused in this Letter on pulsars with small hot spots with opening angles $\delta\theta < 10^{\rm o}$. The extension to big spots is straightforward (§ 3). Note here that the plateau is predicted when both spots are fully visible and the upper limit $A_{\max}$ will remain valid for blackbody emission with antipodal symmetry.

Caps of real pulsars (both radio and X-ray) do not emit as a blackbody and their $I_0(\alpha)$ need not be isotropic. In particular: (1) X-ray pulsars show Comptonized power-law spectra, sometimes along with a clear blackbody component (as in SAX J1808.4-3658). Light bending affects the two components differently: the blackbody pulse from one spot remains sinusoidal while the Comptonized pulse is distorted. This distortion is described by equation (4) and it depends on the anisotropic intensity $I_0(\alpha)$ of the Comptonized emission. (2) For pulsars of high spin (with ms periods) the Doppler effect changes $I_0(\alpha)$. It is easily added to the model by the corresponding transformation of I_0 from the spot rest frame to the local non-rotating frame. (3) A strong magnetic field $B \sim 10^{12}$ G leads to anisotropic emissivity with a preferential direction along the field. In any case, calculations of $I_0(\alpha)$ separate from the light bending effects. Radiation that propagates freely through the pulsar magnetosphere is described by equations (1) and (4) for any $I_0(\alpha)$.

APPENDIX: LIGHT PROPAGATION IN A SCHWARZSCHILD METRIC

For a given photon trajectory let us choose Schwarzschild coordinates $x^k = (t, r, \theta, \psi)$ so that the trajectory is in the plane $\theta = 90^{\rm o}$. Let $u^k = dx^k/d\lambda$ be the 4-velocity of the photon (λ is an affine parameter, $\lambda = r$ at $r \to \infty$). The trajectory has integrals $u_t = 1$ and $u_\psi = b$. From $u^i u_i = 0$ one finds $(u^r)^2 = 1 - (b^2/r^2)(1 - r_g/r)$. Let us choose $\psi = 0$ for the escape direction. Then at radius R the photon has

$$\psi = \int_R^\infty \frac{-u^\psi}{u^r}\, dr = \int_R^\infty \frac{dr}{r^2}\left[\frac{1}{b^2} - \frac{1}{r^2}\left(1 - \frac{r_g}{r}\right)\right]^{-1/2}. \tag{9}$$

The emission angle α (between the emitted photon and the local radial direction) is $\tan\alpha = \sqrt{u^\psi u_\psi}/\sqrt{u^r u_r}$ which yields

$$\sin\alpha = \frac{b}{R}\sqrt{1 - \frac{r_g}{R}}. \tag{10}$$

Combining equations (9) and (10) one can compute numerically the relation between ψ and α for a given R. At small $u = r_g/R$ one can expand equation (9) in u and keep the liner term only. Using the equality $\int_0^{\sin\alpha}(\sin\alpha - z^3)(1-z^2)^{-3/2}dz = 2(1-\cos\alpha)$ one gets $\psi = \alpha + u(1-\cos\alpha)/\sin\alpha + O(u^2)$.

Consider a star of radius R with a surface radiation intensity $I_0(\alpha)$ which can vary over the surface. The observer location is given by a radius-vector $\mathbf{D}$ ($D \gg R$). A (visible) surface element $dS = R^2 d\mu\, d\phi$ is observed at impact parameters $(b, b+db)$ and subtends a solid angle $d\Omega = b\, db\, d\phi/D^2$ on the observer sky. Here $\mu = \cos\psi$ and ϕ is an azimuthal angle corresponding to rotation around $\mathbf{D}$; b depends on μ only, not on ϕ. The observed radiation flux from dS is $dF = I d\Omega$ where $I = (1-r_g/R)^2 I_0$ [I and I_0 are related through $I/\nu^4 = I_0/\nu_0^4$ and the frequency redshift $\nu/\nu_0 = (1-r_g/R)^{1/2}$, see Misner et al. 1973]. Using equation (10) one gets

$$dF = \frac{Ib}{R^2}\left|\frac{db}{d\mu}\right|\frac{dS}{D^2} = \left(1 - \frac{r_g}{R}\right) I_0(\alpha)\cos\alpha \frac{d\cos\alpha}{d\mu}\frac{dS}{D^2}. \tag{11}$$

REFERENCES

Misner, C. W., Thorne, K. S., & Wheeler, J. A. 1973, Gravitation, (San Francisco: Freeman)

Pechenick, K. R., Ftaclas, C., & Cohen, J. M. 1983, ApJ, 274, 846

Shapiro, S. L., & Teukolsky, S. L. 1983, Black Holes, White Dwarfs, and Neutron Stars, (New York: Wiley-Interscience)